Supporting information for:

Safety Assessment of Graphene acid and Cyanographene: Towards New Carbon-based Nanomedicine

Tomas Malina[a], Cordula Hirsch[c], Alexandra Rippl[c], David Panacek[a], Katerina Polakova[a], Veronika Sedajova[a], Magdalena Scheibe[a], Radek Zboril[a,b,*] and Peter Wick[c*]

[a]Regional Centre of Advanced Technologies and Materials, Czech Advanced Technology and Research Institute (CATRIN), Palacký University, Šlechtitelů 27, 779 00 Olomouc, Czech Republic

[b]Nanotechnology Centre, Centre of Energy and Environmental Technologies, VŠB−Technical University of Ostrava, 17. Listopadu 2172/15, 708 00 Ostrava-Poruba, Czech Republic

[c]Empa, Swiss Laboratory for Materials Science and Technology, Laboratory for Particles-Biology Interactions, Lerchenfeldstrasse 5, CH-9014 St. Gallen

[*]Corresponding authors' e-mail: peter.wick@empa.ch , radek.zboril@upol.cz

Number of figures: 6

Number of tables: 2

1. Comprehensive characterization of the materials (GA, GCN, GO)

The size, shape, and height of GFMs' sheets were characterized using transmission electron microscopy (TEM, JEOL 2100 operating at 160 kV) and atomic force microscopy (AFM). For AFM, combined system NTEGRA Spectra (NT-MDT) was utilized to acquire sample topography (software Nova Px. 3.4.0 rev. 19040). ImageJ software was used to measure at least 200 sheets for each material to determine the size and height distribution of the GA, GCN and GO sheets. The surface morphology was obtained by the means of semi-contact mode (height) with an ACTA-SS (AppNano) cantilever having a force constant of 13-77 N/m and resonant frequency of 200 – 400 kHz. The scanning rate was 0.5 Hz. During the measurement the humidity was in range of 25-35% and the temperature was RT. The height profile and surface roughness (RMS) was calculated using Gwyddion 2.51 software. To determine the surface chemistry, materials were characterized with spectroscopy techniques: X-ray photoelectron spectroscopy (XPS), Fourier transform infrared spectroscopy (FTIR) and Raman spectroscopy. XPS data were measured using a PHI VersaProbe II (Physical Electronics) spectrometer, using Al Kα source. The XPS spectra were fitted using the MultiPak (Ulvac – PHI, Ind.) software package. All binding energies were referenced to the carbon C 1s peak (284.4 eV peak). FTIR spectra were obtained with an iS5 Thermo Nicolet spectrometer (with ZnSe ATR technique) and Raman spectra using a DXR Raman microscope. Additionally, zeta potential of studied materials was determined by Zetasizer Nano Zs (Malvern). The additional results are shown in the Figure S1 for size and height sheet characterization and Figure S2 for surface chemistry characterization of GA, GCN and GO samples.

It can be seen that there are differences between materials derived from graphite fluoride (GF) (GCN and GA) and GO, which is usually prepared by oxidation of graphite. GF-derived materials consisted of few- to multi-layered sheets of small lateral sizes (majority of sheets under 500 nm, Figure S1b and S1c). GO sample on the other hand contained mostly single-layered sheets of slightly higher size (majority of sheets under 1000 nm, Figure S1b and S1c). It needs to be mentioned though that GO also showed a higher heterogenity in size, as low percentage of bigger (> 1000 nm) sheets was also detected (Figure S1b).

X-ray photoelectron spectroscopy (XPS) analysis shows major presence of carbon and oxygen for GA and GO, with the nitrogen content higher for the GCN sample originating from the cyano-functional groups (Figures S2a and S2b). The deconvoluted C 1s domain of the high-resolution XPS (HR-XPS, Figure 1b) spectra showed that GCN consisted mostly of sp^2 and sp^3

carbons, with major component of C-N bond, corresponding to the cyano-functional groups. Acidic hydrolysis afforded the GA product, as described in previously published reports [1-3], where the oxygen content increased from 5.5 at% to 17.9 at% and nitrogen decreased to 3.2 at%. As a comparison material to two well-defined graphene derivatives, the GO sample was also analyzed by the XPS technique, revealing much higher oxygen content coming from the various oxygen configurations on its surface, in contrast with GA homogenous coverage of carboxylic groups (Figure 1b).

Intense C≡N vibration was found at 2250 cm^{-1} in GCN FTIR spectrum, confirming its high functionalization degree with cyano groups (Figure 1c). By the acidic hydrolysis, this has been transformed into 1700 cm^{-1} feature of carbonyl (C=O) vibration of the carboxyl groups of the GA (Figure 1c). This feature was observable also in GO signifying presence of carbonyl or carboxyl groups (Figure 1c). Fingerprint regions of all the spectra consisted of many vibration modes that manifest as two broad bands with two main maxima at around 1550 cm^{-1} assigned mainly to skeletal aromatic C=C vibrations, and around 1200 cm^{-1} related to the rest of the skeletal C-C vibrations in the vicinity of defects. The latter band was much weaker and less resolved in the case of GO. Moreover, in GO, additional feature is observable at around 1050 cm^{-1} possibly related to C-O vibrations of alkoxy and epoxy groups that of GO. In GCN, there were signs of aliphatic C-H vibrations not observable in GA or in GO. In the case of GA synthesized from GCN, this is possibly due to the fact, that the side chains are cleaved by oxidizing agent and transformed also into carboxyl groups. All the materials exhibited strong and very broad signal between 3000-3700 cm^{-1} assigned to O-H stretching vibrations. In the case of GO and GA, both materials contain O-H groups either as part of carboxyl groups or, in the case of GO, in alkoxy groups alone. The broadness of the signal stems from the possible hydrogen bonding between the groups on the same or different sheets of GO and GA. Since the FTIR spectra were recorded by drop-casting the aqueous dispersion of the materials onto the ATR accessory crystal, residual water molecules bound to the GO and GA surface through the hydrogen bonding may also contribute to the intensity of the signal. This reasoning also applies for GCN that does not have OH groups except of their possible presence caused by side-processes during the GCN synthesis. CN groups also may participate in hydrogen bonding with residual water molecules of the aqueous dispersion, hence the detected strong OH band.

The Raman spectra of all materials (Figure S2c) showed G bands found at 1595 cm^{-1}, indicating the presence of well-developed graphene sp^2 regions, however, in the cases of GCN and GA,

unlike GO, the D band found at 1330 cm^{-1} dominated, which can be consequence of higher number of defects in the graphene structure of GCN and GA. The I_D/I_G ratio gets lower after transforming GCN into GA possibly due to removal of defective sites with aliphatic chains by oxidation with HNO_3. Low I_D/I_G ratio of GO is probably caused by larger size of its sheets, since the graphene edges can also contribute to the D-band intensity.

Since we were using the models of immune and endothelial cells, we assessed the endotoxin contamination of the studied materials using LAL assay (ThermoFisher) according to the manufacturer instructions. There was no significant endotoxin content detected for GA and GCN, on the other hand, concentration of over 0.5 EU/ml was measured for GO sample (Figure S2d). However, since GO was purchased commercially for this study, we took this result into consideration and proceeded with this material for the cellular studies.

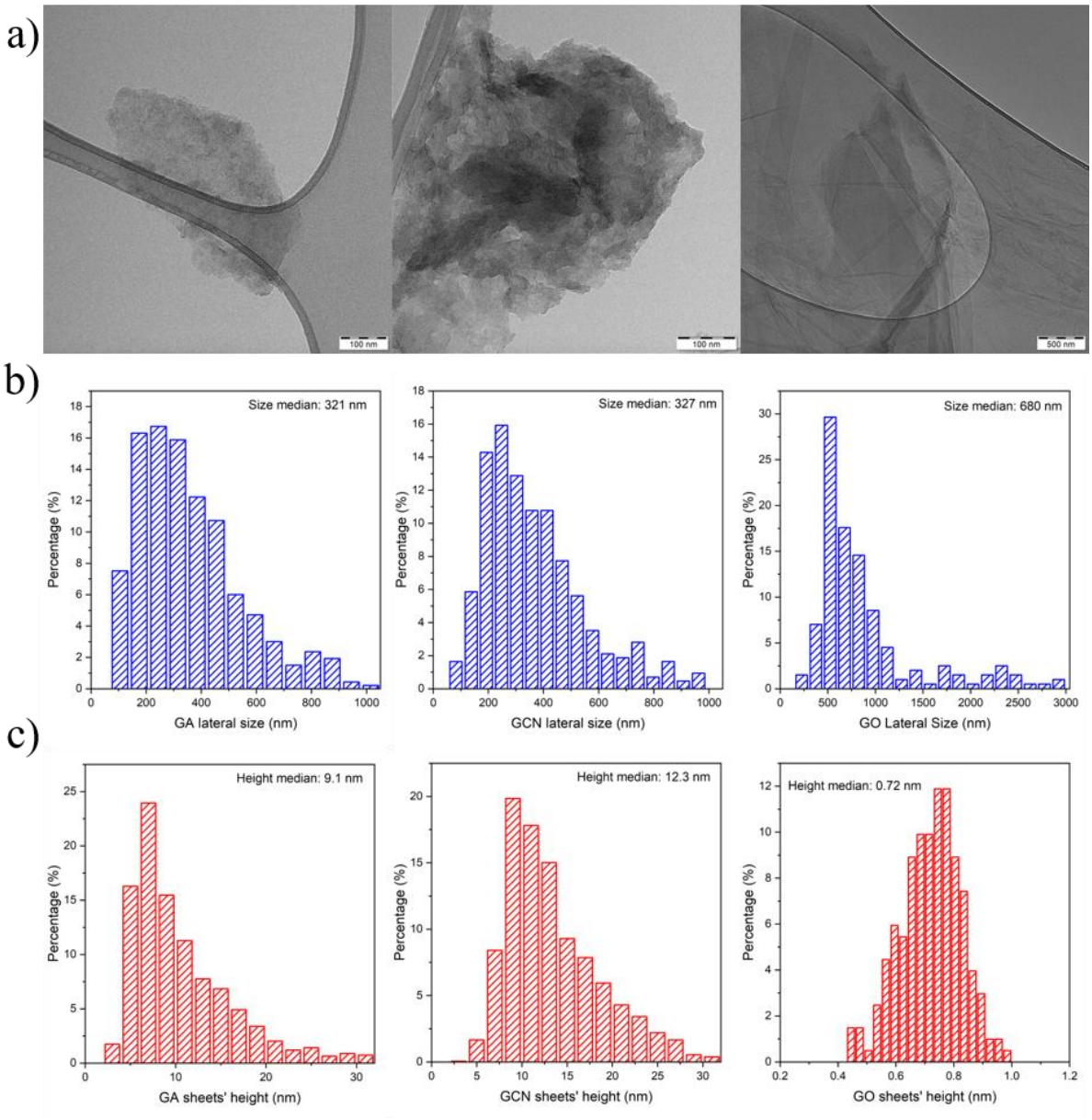

Figure S1. Additional size and height characterization of GA, GCN and GO samples. a) Representative images of (from left to right): GA, GCN and GO. Sheet c) lateral size and d) height distribution of (from left to right): GA, GCN and GO. At least 200 values were recorded for sheet height or size of studied materials.

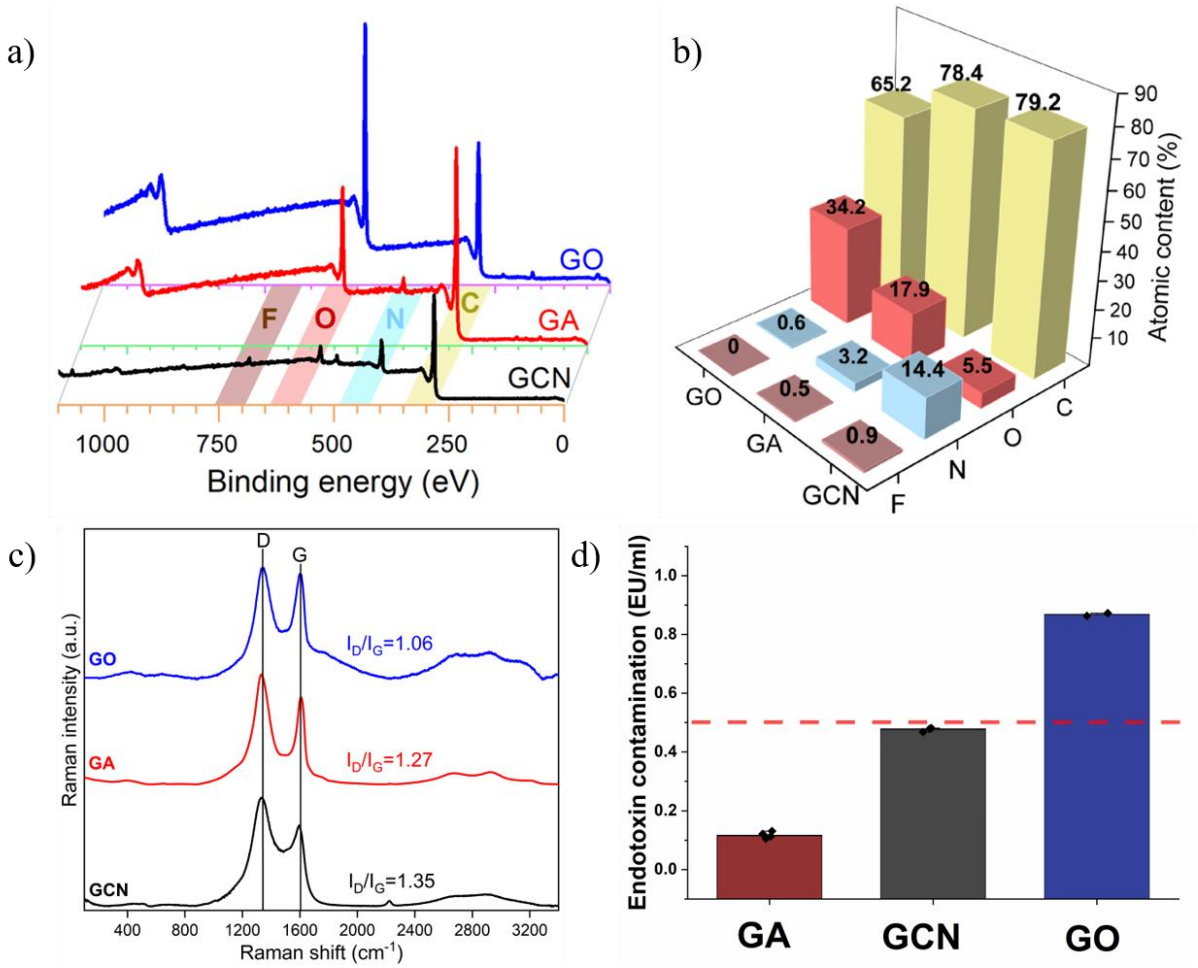

Figure S2. Additional surface chemistry characterization and endotoxin contamination assessment. a) XPS survey spectra, b) Bar graph with atomic compositions. c) Raman spectra, and d) endotoxin contamination expressed in EU/ml units of GA, GCN and GO materials.

2. *Long-term colloidal stability of GA and GCN in complete RPMI-1640 and EGM medium*

For the long-term colloidal stability analysis of studied materials, DLS measurements with Zetasizer Nano Zs instrument (Malvern) and the results showing Z-Average and PdI values are presented in the Figure S3. For the experiment, the suspensions were made in the Eppendorf tube and for measurement in various time points (up to 7 days), the 1 ml was transferred to the cuvette and DLS data were obtained. The results clearly show that both GA and GCN form stable colloids even after 7 days in both complete RPMI-1640 and EGM.

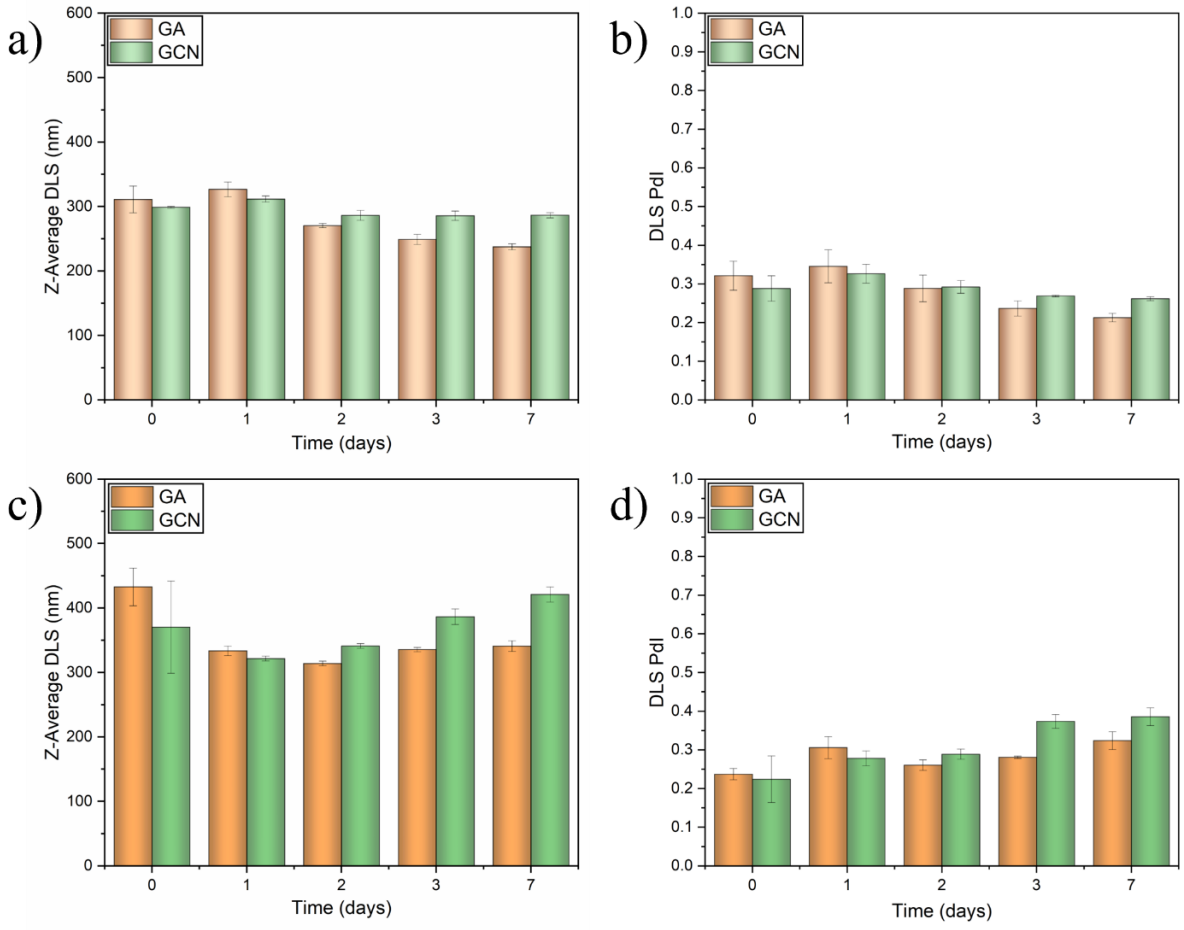

Figure S3. Long term colloidal stability of GA and GCN samples in a) and b) complete RPMI-1640 and c) and d) complete EGM culture medium by DLS. a) and c) Z-Average values of studied materials incubated in two culture media for several time points up to 7 days. b) and d) PdI values of studied materials incubated in two culture media for several time points up to 7 days.

3. Interference controls for LDH and Alamar blue assays

To check the possible interference of GA, GCN and GO with LDH and Alamar blue assays, acellular experiment was conducted. Briefly, for the LDH assay, 50 µl of suspensions containing the investigated concentrations (0 to 30 µg/ml) were transferred in the 96 well-plate and then LDH assay was conducted. The absorbance values detected at 490 nm are displayed in the Figure S4a. For the alamar blue assay, resorufin sodium salt (Sigma, fluorescent dye compound in the Alamar blue assay) was added diluted in the complete RPMI-1640 (final c 5 µg/ml) to the 50 µl of acellular suspensions containing the investigated concentrations (0 to 30 µg/ml) and fluorescence was measured using microplate reader with setup: ex. 540/em. 590 nm

(Mithras2 Plate reader, Berthold Technologies) (Figure S4b). We can see from the measured values that in the used concentration range, only the highest concentration of GA and GCN (30 µg/ml) is causing only modest interference with both assays. We detected small increase in the absorbance, while the fluorescence of resorufin was slightly decreased. Even though the these results showed very low or none interference effect in the tested concentrations, we always included the acellular controls with the cellular experiments and were observing any unusual increase in LDH absorbance or decrease in alamar blue fluorescence.

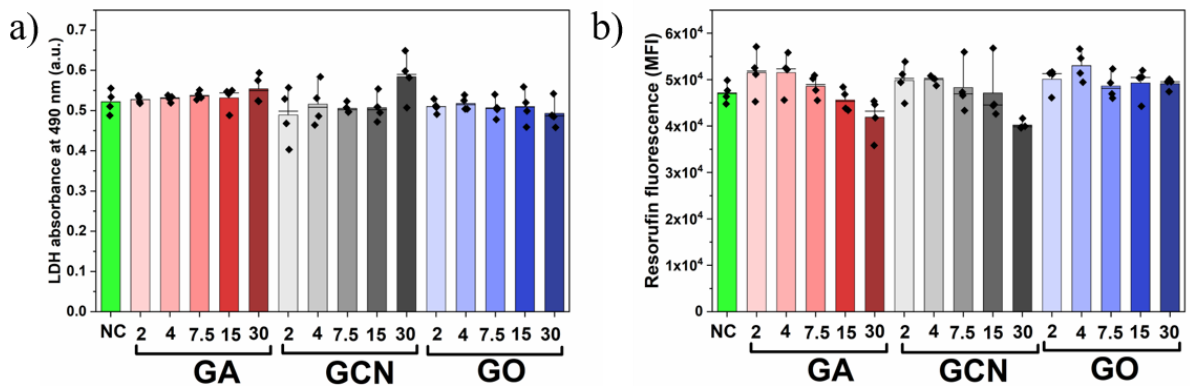

Figure S4. a) absorbance values for acellular controls of various concentrations of GA, GCN and GO prepared in complete RPMI-1640 media. b) Mean fluorescence intensity (MFI) values for for acellular controls of various concentrations of GA, GCN and GO prepared in complete RPMI-1640 media in presence of resorufin sodium salt in final concentration 5 µg/ml.

4. Elisa for TNF-α release after of THP-1 (undifferentiated, differentiated) and HUVECs treated with GA, GCN, and GO for 24 h

Even though we measured TNF-α release using two time-points (6 and 24 h), we found that 24 h is already too late as level of TNF-α comparable to the untreated sample was detected in the supernatant of undifferentiated THP-1 and HUVECs in the positive control sample with 1 µg/ml of LPS. For differentiated THP-1 cells, although we have detected significantly higher levels of TNF-α then in control untreated sample, the concentration was again significantly lower than in the experiment after 6 h.

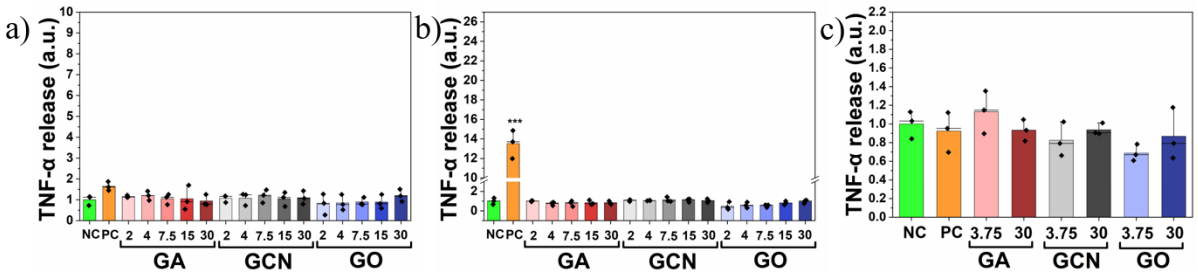

Figure S5. TNF-α release of a) undifferentiated THP-1, b) differentiated THP-1 and c) HUVECs treated for 24 h with various concentrations of GA, GCN and GO. Statistics was done using one way anova with Dunnet post hoc vs control untreated sample (* $p \leq 0.05$, ** $p \leq 0.01$, *** $p \leq 0.001$). Scales on y axis are the same as for results after 6 h shown in Figures 3 and 4.

5. *Images of complete shear-ring co-culture model after 24 h of treatment with 30 µg/ml of GA, GCN and GO under flow*

To further highlight the difference in the colloidal stability between our novel derivatives GA and GCN and benchmark derivative GO, we took pictures of the complete shear rings treated with 30 µg/ml of GA, GCN and GO under flow for 24 h (Figure S6). From the images below, we can see that GA and GCN remained in the nice colloidal suspensions even after 24 h under flow in the shear-ring confirming their excellent colloidal behavior. On the other hand, GO sample after 24 h under flow in complete EGM formed a huge agglomerates that were clearly visible floating on top of the culture medium (Figure S5d). This finding was not that surprising given that we already showed a very poor GO colloidal stability in complete EGM before. However, this behavior resulted in a completely different exposure of this sample to cells, as it was no longer GO sheets in contact with the tested cells, but very big agglomerates. For this reason, we excluded the GO sample from the further adhesion assay experiment.

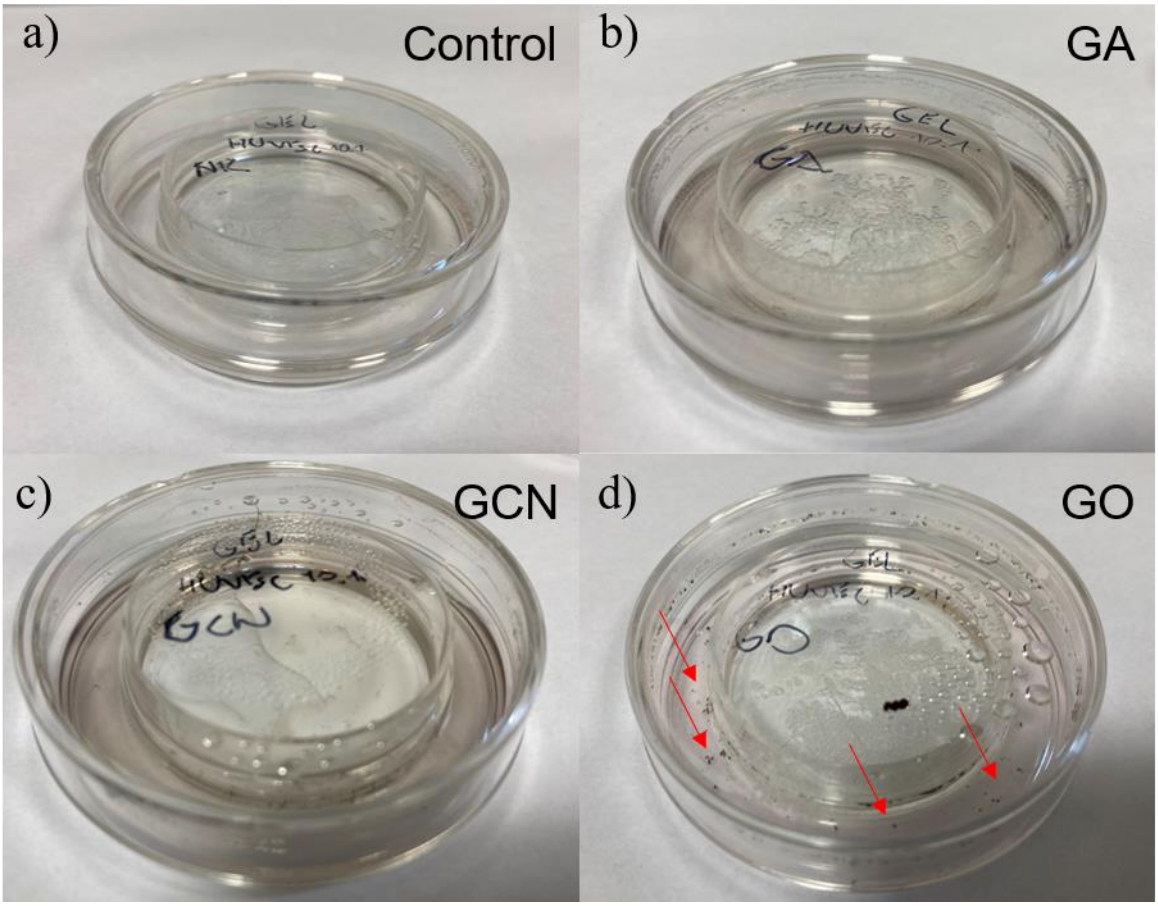

Figure S6. Representative images of HUVECs + THP-1 cells in Shear-ring model treated for 24 h with studied materials: a) untreated control, b) GA 30 µg/ml, c) GCN 30 µg/ml and d) GO 30 µg/ml. Red arrows highlighting the material agglomerates forming only for GO sample due to its poor colloidal stability in complete EGM culture medium.

Table S1: Complete RPMI-1640 medium supplementation (Sigma Aldrich):

Components	**Concentration (g/l)**
L-Arginine (Free Base)	0.2
L-Asparagine (Anhydrous)	0.05
L-Aspartic Acid	0.02
L-Cystein•2HCl	0.0652
L-Glutamic Acid	0.02
L-Glutamine	0.3
Glycine	0.01
L-Histidine (Free Base)	0.015

Hydroxy-L-Proline	0.02
L-Isoleucine	0.05
L-Leucine	0.05
L-Lysine•HCl	0.04
L-Methionine	0.015
L-Phenylalanine	0.015
L-Proline	0.02
L-Serine	0.03
L-Threonine	0.02
L-Tryptophan	0.005
L-Tyrosine•2Na•2H_20	0.02883
L-Valine	0.02
Biotin	0.0002
Choline Chloride	0.003
Folic Acid	0.001
Myo-Inositol	0.035
Niacinamide	0.001
D-Pantothenic Acid Hemicalcium	0.00025
PABA	0.001
Pyridoxine•HCl	0.001
Riboflavin	0.0002
Thiamine•HCl	0.001
Vitamin B12	0.000005
Calcium Nitrate•4H_20	0.1
Magnesium Sulfate (Anhydrous)	0.04884
Potassium Chloride	0.4
Sodium Chloride	6.0
Sodium Phosphate Dibasic (Anhydrous)	0.8
D-Glucose	2.0
Glutathione, Reduced	0.001
Phenol Red•Na	0.0053
Fetal Bovine Serum	100

175

Table S2: Complete EGM medium supplementation (Promocell):

Component	Concentration
Fetal Calf Serum	0.02 ml/ml
Epidermal Growth Factor (recombinant human)	5 ng/ml
Basic Fibroblast Growth Factor (recombinant human)	10 ng/ml
Insulin-like Growth Factor (R3 IGF-1)	20 ng/ml
Vascular Endothelial Growth Factor 165 (recombinant human)	0.5 ng/ml
Ascorbic Acid	1 µg/ml
Heparin	22.5 µg/ml
Hydrocortisone	0.2 µg/ml

References:

[1] A. Bakandritsos, M. Pykal, P. Błoński, P. Jakubec, D.D. Chronopoulos, K. Poláková, V. Georgakilas, K. Čépe, O. Tomanec, V. Ranc, A.B. Bourlinos, R. Zbořil, M. Otyepka, Cyanographene and Graphene Acid: Emerging Derivatives Enabling High-Yield and Selective Functionalization of Graphene, ACS Nano 11 (2017) 2982-2991. https://doi.org/10.1021/acsnano.6b08449.

[2] V. Sedajova, P. Jakubec, A. Bakandritsos, V. Ranc, M. Otyepka, New Limits for Stability of Supercapacitor Electrode Material Based on Graphene Derivative, Nanomaterials 10 (2020) 1731. https://doi.org/10.3390/nano10091731.

[3] I. Obraztsov, A. Bakandritsos, V. Sedajova, R. Langer, P. Jakubec, G. Zoppellaro, M. Pykal, V. Presser, M. Otyepka, R. Zboril, Graphene Acid for Lithium-Ion Batteries-Carboxylation Boosts Storage Capacity in Graphene, Adv. Energy Mater. 12 (2022) 2103010. https://doi.org/10.1002/aenm.202103010.